COMPARISON OF THE EFFECTS OF A CONVENTIONAL HEAT TREATMENT BETWEEN CAST AND SELECTIVE LASER MELTED IN939 ALLOY

W. Philpott, M. A. E. Jepson, R. C. Thomson
Department of Materials, Loughborough University,
Loughborough, Leicestershire, LE113TU, UK

ABSTRACT

Additive manufacturing (AM) is a process where, as the name suggests, material is added during production, in contrast to techniques such as machining, where material is removed. With metals, AM processes involve localised melting of a powder or wire in specific locations to produce a part, layer by layer. AM techniques have recently been applied to the repair of gas turbine blades. These components are often produced from nickel-based superalloys, a group of materials which possess excellent mechanical properties at high temperatures. However, although the microstructural and mechanical property evolution during the high temperature exposure of conventionally produced superalloy materials is reasonably well understood, the effects of prolonged high temperature exposure on AM material are less well known.

This research is concerned with the microstructures of components produced using AM techniques and an examination of the effect of subsequent high temperature exposures. In particular, the paper will focus on the differences between cast and SLM IN939 as a function of heat treatment and subsequent ageing, including differences in grain structure and precipitate size, distribution and morphology, quantified using advanced electron microscopy techniques.

INTRODUCTION

Additive manufacturing has been gaining popularity in recent years as a method for the manufacture of gas turbine components due to the efficiency of the process, and the ability to produce complex designs for improved performance, which would be difficult, time-consuming and expensive to produce using conventional techniques (1–3). This is becoming increasingly more important with the hollow structures and cooling channels present in modern turbine components (4). One popular additive manufacturing technique is Selective Laser Melting (SLM) where a laser selectively scans over powder which is melted and fused layer by layer to build up a part. This process creates large temperature gradients which lead to residual stresses in the solidified material (5–9). This rapid cooling also means that there is no time for precipitates to form. Epitaxial growth of grains through the build layers is achieved by partial remelting of previous layers (10).

Many turbine component alloys require pre-service heat treatments to achieve a very specific microstructure for optimal performance in service. In some cases, when a component has been additively manufactured, the conventional heat treatments are simply applied to this material even though it is produced in a different way. However, these heat treatments have been designed

to achieve the desired microstructure from very specific starting microstructures and have been optimised for conventionally produced material.

As the microstructure of additively manufactured material is very different to conventionally produced material (e.g. by casting), it is important to study the effects of the heat treatment, because it's influence on the microstructure of additively manufactured material is relatively unknown and not well studied (11,12). A cast material will generally have large, relatively equi-axed grains, and in the case of turbine component materials, large discrete carbides which have formed on grain boundaries in the material(13). In contrast to this, the grains in material produced using SLM, are very fine, high aspect ratio and columnar, and extend through the microstructure in the build direction(14). There is significant grain orientation in the material as a result of the process(10) and any precipitation is effectively suppressed, leaving a supersaturated solution of the matrix(15).

Nickel-based superalloys are the group of materials generally used for gas turbine components due to their ability to function at temperatures up to $0.8T_m$ (1,16) and maintain their mechanical properties. One such alloy is Inconel(IN)939, a high-chromium alloy with good mechanical properties which is capable of operating at temperatures up to 850°C for long periods of time (17). IN939 is strengthened by both gamma prime (γ') precipitates and carbides. When produced by casting, the MC carbides in the alloy are generally large and discrete, whereas the $M_{23}C_6$ carbides are much smaller (18). These carbides both prevent movement of dislocations and sliding of grain boundaries, which can be common above $0.5T_m$ (15,19).

A heat treatment is applied to IN939 components before they enter service to achieve a number of things: firstly for stressed applications, a hot isostatic pressing (HIP) step can be used to reduce porosity, as is used with other alloys (20). This step can be especially beneficial for SLM-produced material as it can be prone to cracking and porosity (21,22), which HIP has been shown to effectively remove (23). Next is a high temperature solution treatment step, designed to dissolve the gamma prime precipitates present in the as-cast state back into solution, so that the size and morphology of the precipitates can be controlled more effectively in the subsequent aging steps. The conventional heat treatment for IN939 then usually involves a single aging step (24) to coarsen the γ' precipitates and achieve the desired cuboidal shape which is the optimal morphology for creep performance (1).

This paper will focus on a comparison of the effects of the conventional 1 step age heat treatment and a slightly altered heat treatment involving a 3 step age on the microstructure of IN939 produced by both SLM or casting. By examining the differences in the effects of the heat treatments between material produced by the two processes it will be possible to determine if the desired pre-service microstructure is achieved in the SLM-produced material and thus whether the conventional heat treatment is suitable for material produced in this way, or if the heat treatment should be altered to better achieve the desired microstructure.

EXPERIMENTAL METHODS

Material

The nominal composition of IN939 is given below in Table 1.

Table 1: Nominal composition of IN939 alloy (25)

Material	Ni	Cr	Co	W	Ta	Nb	Al	Ti	C	B	Zr
IN939	Bal.	22.5	19	2	1.4	1	1.9	3.7	0.15	0.009	0.09

SLM Samples were built using an EOS M270 machine with argon gas flushing, with a laser power of 195 W. The as-produced SLM material was received in two batches, the first batch was in the form of an 80 mm long 10 mm diameter cylindrical bar built horizontally. The second batch was another cylinder of 12 mm diameter built vertically. The cast material was received in the form of cuboidal ingots 50x10x15 mm; these were all cut into 10 mm long sections to be used in this study.

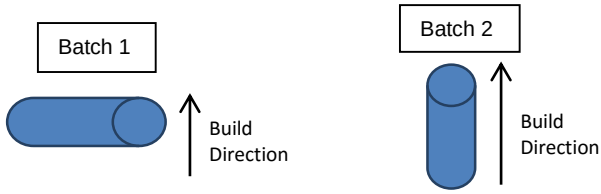

Figure 1: Diagrams showing build directions in the different batches of SLM material

Preparation

The as-produced material was cut in two different orientations as shown in Fig. 2 using an aluminium oxide cut-off wheel, with ample cooling and a maximum cutting speed of 0.008 mms^{-1}. No significant differences were found between orientations in the cast material, so for later samples only one orientation was used. In the SLM material the direction of one of the cuts was chosen to intersect the build layers in the material so that a cross section of the build layers could be seen, and the second cut was used to effectively bisect a single build layer.

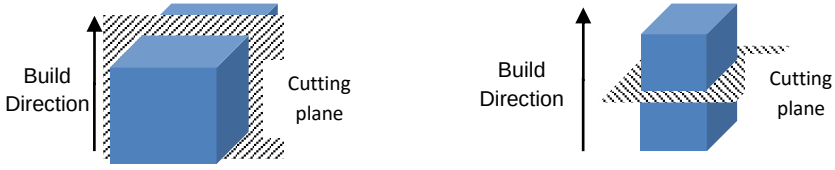

Figure 2: Diagrams showing first and then second cutting directions for initial cast samples and all SLM samples with the build direction shown for SLM samples.

Heat Treatment

The traditional heat treatment for the material involves a high temperature hot isostatic pressing (HIP) step, followed by a slightly lower temperature solution treatment step, which is then usually followed by a single longer aging step at lower temperature. However, the heat treatment with a single aging step can lead to some brittleness in the fully heat treated material (11), therefore a heat treatment with three separate aging steps at successively lower temperature can be used to improve ductility. Both methods are compared in this study.

Samples were heat treated in a manually controlled furnace, with a sample of cast and SLM material removed after each step to obtain a sample in the condition of each different step of the heat treatment. A HIP heat simulation step was used to simulate the heating of the HIP step without the pressure, to focus on the effect of the temperature on the material during this step.

Analysis

Samples were mounted in electrically conductive Bakelite and polished to 1 µm using successively finer grades of SiC pads and polishing pads with diamond suspension. A final (0.05 µm) colloidal silica polishing step was then used. Backscattered electron imaging was used for all samples, which was performed using a Hitachi tungsten filament scanning electron microscope (SEM) and a Jeol field emission gun scanning electron microscope (FEGSEM). Transmission electron microscope (TEM) samples were prepared using an FEI NovaNanolab dual beam system with a focused ion beam (FIBSEM). Energy dispersive x-ray spectroscopy (EDS) was performed in the FEGSEM and a TECNAI scanning transmission electron microscope (STEM) to analyse the chemical composition of phases and precipitates. A Jeol conventional transmission electron microscope (TEM) was used for imaging of precipitates and for diffraction to identify precipitates. In order to examine the γ' structure of the samples they were electrolytically etched at 3V using hydrofluoric acid as the etchant for 3-5 seconds. These samples were then imaged using the FEGSEM. Image analysis to quantify precipitates was performed using the ImageJ image analysis software. Precipitates were highlighted using image thresholding and the software was then used to analyse size, area percentage and counts. A number of areas were analysed in each sample, the precipitates were highlighted and quantified, and then the data were averaged.

RESULTS AND DISCUSSION

As-produced Material

The as-produced material is high density (99%+) and is very typical of material produced by the two processes. As shown in Fig. 3; the cast material consists of large equi-axed grains, while the SLM-produced material has very fine high aspect ratio columnar grains. There are large (~5 µm^2) precipitates visible in the cast microstructure, whereas in the SLM material only extremely small precipitates (less than 50 nm) have formed, as shown by the higher magnification inset on b).

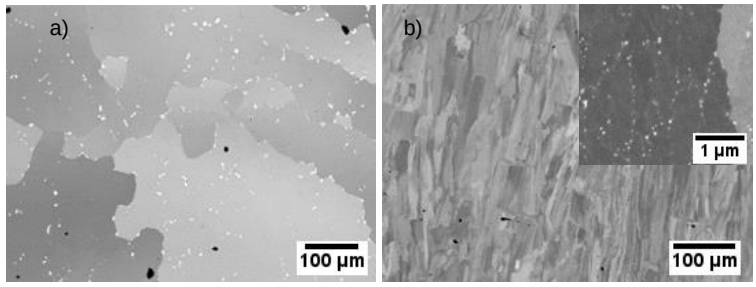

Figure 3: Backscattered electron images showing microstructure of IN939 samples in the as-manufactured state produced by a) Casting and b) SLM

Microscopy of Heat Treatment Stages

The changes occurring in the microstructure of both the cast and SLM-produced samples through the heat treatment steps are shown in Fig. 4. For the cast material there are no apparent changes to the microstructure throughout the heat treatment steps observable in the SEM. Changes in the γ' precipitate size and distribution are not visible here, but will be discussed in a later section. The

SLM-produced material, however, shows extensive recrystallization throughout the course of the heat treatment, which progresses through each step until in the fully heat treated materials, almost all the fine columnar grains have been replaced with much larger, lower aspect ratio grains.

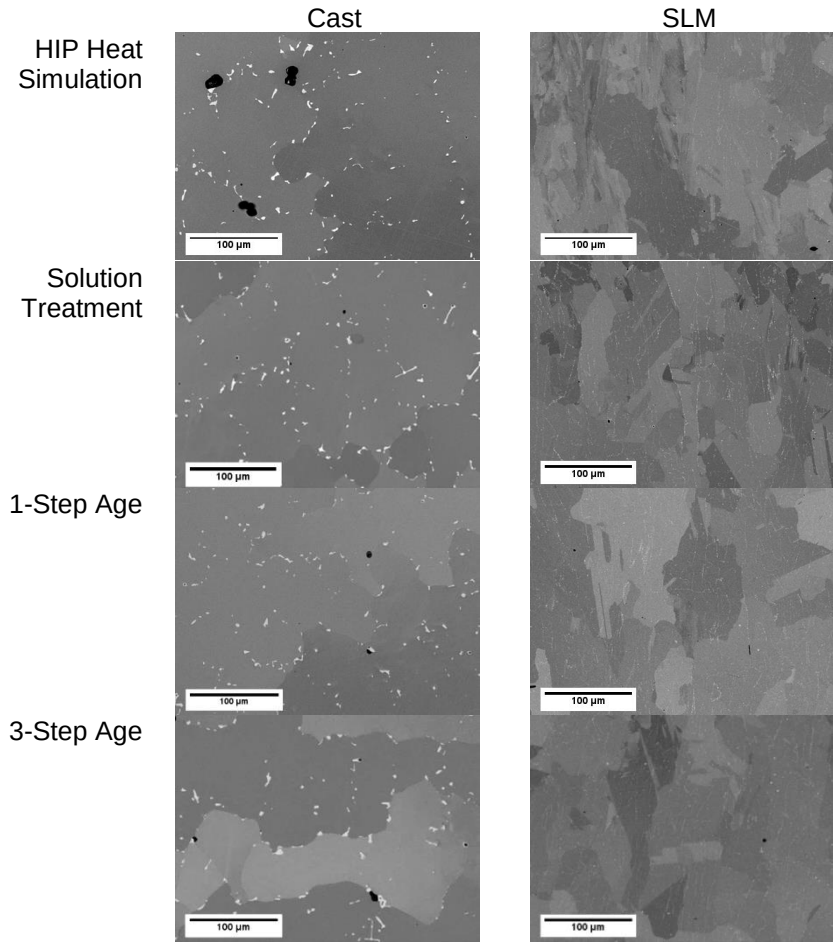

Figure 4: Backscattered electron images of Cast and SLM material after the heat treatment processes

The other visible difference in the SLM material is the appearance of bright precipitates large enough to be visible at this magnification after the HIP heat simulation step. While the precipitates in the cast material are large (~5 μm^2) and spaced far apart (10 µm+ separation between carbides), the precipitates in the SLM-produced material are very small (~0.5 μm^2) and spaced very close together (~1 µm separation). Based on the size, contrast and location of these precipitates, they appear to be MC type carbides(13,19), however, it is necessary to confirm this. Using EDS mapping, these precipitates were found to be very rich in titanium and rich in carbon, as shown in Fig. 5.

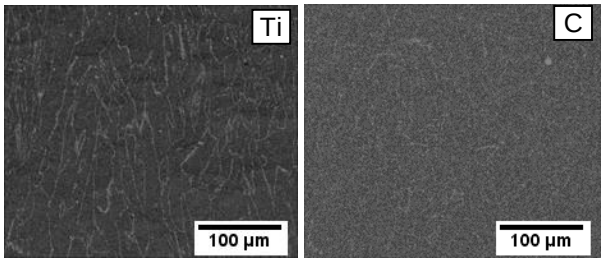

Figure 5: EDS maps showing precipitates are rich in titanium and carbon

The EDS was then performed with point analysis using atomic percentage to show the precipitates are ~50 % carbon and very rich in titanium. TEM electron diffraction (as shown in Fig. 6) then confirmed that these precipitates are MC carbides.

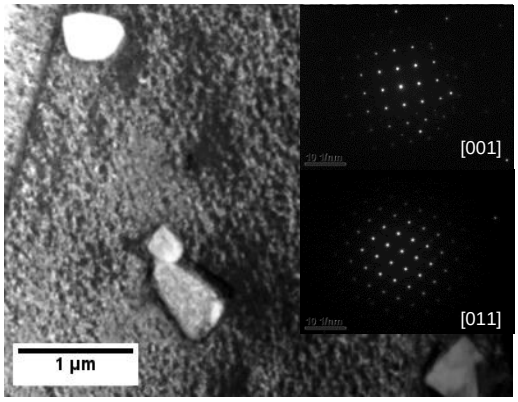

Figure 6: TEM image of carbides in fully heat treated (1-step age) IN939 along with electron diffraction patterns obtained from these carbides

There were also some small dark precipitates on grain boundaries in the fully heat treated materials which appeared to be $M_{23}C_6$ carbides. This observation is supported by EDS data which gave a carbon content of ~20 at.% and a chromium content of ~50 at.% which, when accounting for carbon contamination and beam interaction with the surrounding matrix, are around the values expected of $M_{23}C_6$ carbides (26). Compared to the MC type carbides these are very few in number so will not be the focus of this paper. Based on the pattern of precipitation of the MC carbides in the SLM material it seems that they formed very early in the heat treatment on the pre-existing grain boundaries. As the material has recrystallised, these precipitates have remained in place, but are no longer on grain boundaries, as can be seen more clearly in Fig 7.

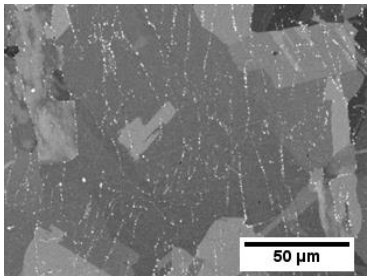

Figure 7: Backscattered image of solution treated SLM-produced IN939 viewed parallel to the build direction, showing a small number of precipitates on recrystallized grain boundaries and others aligned with original grain boundaries inside recrystallized grains.

The reason for these changes is that in the as-produced state, the SLM-produced material is a supersaturated solution, with a large amount of residual stress and stored energy (6,15), so when heat is applied, there is a large driving force for recrystallisation as a method of stress relaxation. Therefore, throughout the course of the heat treatment the microstructure changes from a very fine columnar microstructure into a more coarse-grained microstructure, with lower aspect ratio grains. However, although there is a great deal of recrystallization and grain growth, it is noted that the grain size in the SLM material still remains much smaller than the cast material.

With the carbides the situation is similar: with a supersaturated microstructure there is a large driving force for formation of precipitates in the matrix, coupled with the fact that the repeated heat input of the successively melted layers throughout the SLM process can be sufficient to produce nuclei for precipitates (11), this means that when heat is applied very small and closely distributed precipitates form very rapidly. Throughout the heat treatment process it is not possible to accurately determine visually what is happening to the carbides, therefore image analysis was used to quantify this.

Carbide Quantification

The difference in effect of the heat treatment steps on the carbides in the cast and SLM-produced material is very noticeable from the quantification shown in Fig. 8 and Fig. 9. The carbides in the heat treated SLM-produced material are extremely small, but there are many more of them when compared to the cast material. However, although broadly similar, the area fraction is slightly higher in the SLM material, but the trend between both materials throughout the heat treatment is also quite similar, with significant redissolution of carbides occurring during the HIP step, as shown by the decreasing area fraction and counts.

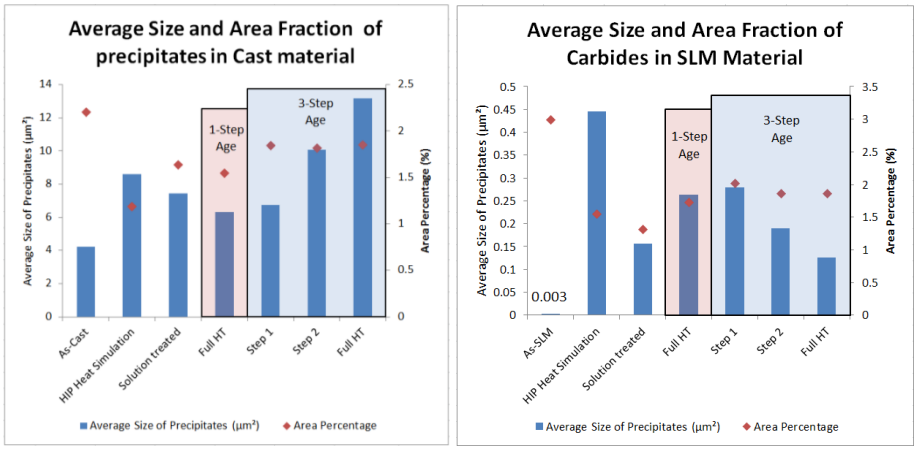

Figure 8: Graphs showing Average Size and Area Percentage of MC carbides in Cast and SLM material throughout the heat treatment process

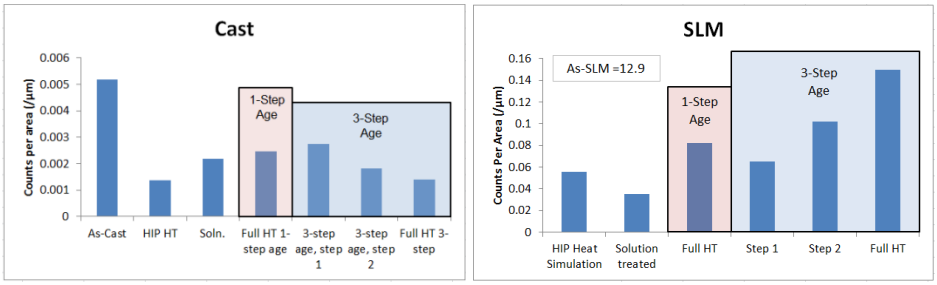

Figure 9: Graphs showing number of carbides per area in SLM and cast material throughout the heat treatment process

The most important result to note from these data, however, is the difference in trend of the counts per area: whereas in the cast material the carbides are coarsening throughout each stage of the 3-step aging process (as shown by the decreasing count and increasing size with constant area percentage), in the SLM material the opposite is occurring and carbides are continuing to precipitate up until the end of the heat treatment. This has important implications as it means that the SLM material is likely to behave differently in service and carbides could continue to precipitate. The presence of these carbides may increase creep performance to an extent (15), but it has previously been shown that too many carbides distributed evenly through the microstructure could cause embrittlement (12). Based on these results it may be necessary to design a different heat treatment procedure for SLM materials compared to cast materials to produce a similar starting microstructure.

Gamma Prime Analysis

The images of the etched samples in Fig. 10 showing the size and morphology of the gamma prime precipitates show that there is not much difference in them between the cast and SLM samples. The precipitates are larger in the cast material after the solution treatment step, however in the fully heat treated samples, the gamma prime precipitates in the SLM-produced sample are very similar in size to those in the cast material in the 1-step aged condition and slightly larger in the 3-step aged condition. After 1-step aging, the precipitates in the SLM-produced material also

appear to have a more complex morphology than those in the cast material as shown by the inset in Fig. 10, which suggests that they may be further evolved than those in the cast material and formed what are described as ogdoadically diced cubes (1), where a cuboidal precipitate partially splits into 8 smaller precipitates. This could be due to the as-produced microstructure having a large amount of stored energy and being a supersaturated solution, therefore having a greater driving force for formation and evolution of the precipitates during the heat treatment (11). However, as there appear to be some instances of a similar morphology in the solution treated samples it may simply be that the precipitates in the cast material have undergone significant coarsening, leaving larger, more simple-shaped precipitates, whereas the precipitates in the SLM material have not.

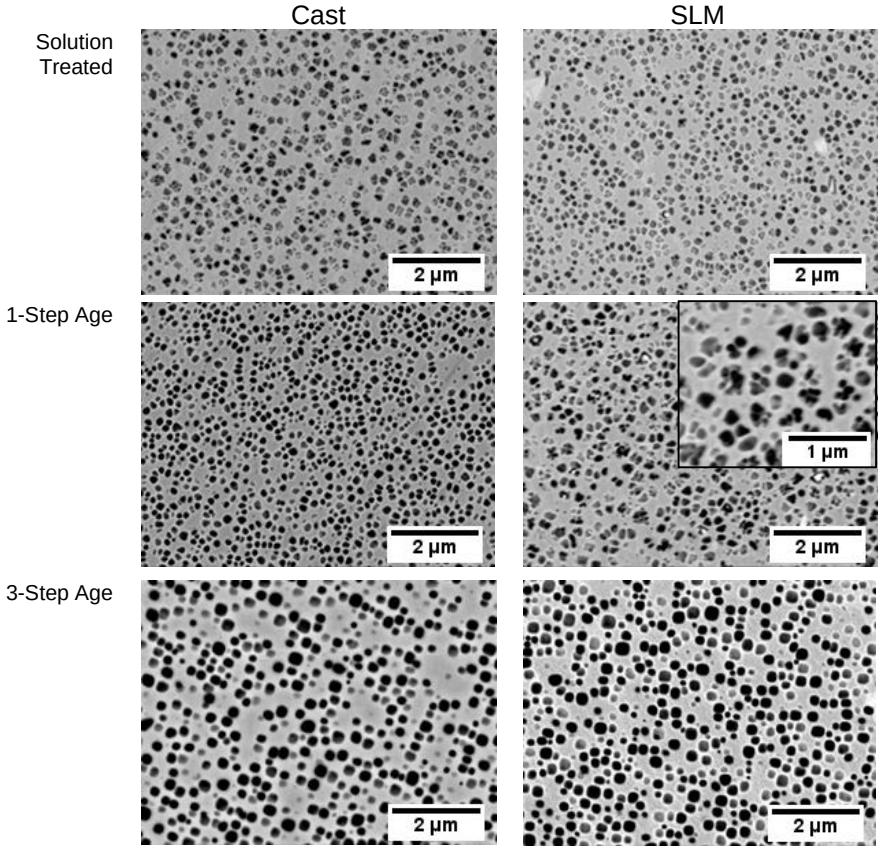

Figure 10: Backscattered electron images showing voids left by gamma prime precipitates in etched IN939 samples through the heat treatment

In the 3-step aged SLM-produced sample, the size and morphology appear to be quite optimal for a pre-service microstructure as the precipitates are large and cuboidal in shape, however there is a possibility that the cuboidal precipitates have also begun to evolve to a more complex shape, so possibly a shorter heat treatment could be beneficial.

Gamma Prime Quantification

The graphs in Fig. 11 illustrate the quantification of γ' in both the cast and SLM samples. It can be seen that both materials follow very similar trends during the heat treatment, except that there appears to be a slightly greater area percentage of γ' in the SLM-produced material in general, and the precipitates are largest in the 3-step aged SLM-produced material. The formation of ogdoadically diced cubes will have reduced the average size of the precipitates in the 1-step aged SLM-produced material, hence why the average size appears slightly lower than in the cast material and the number of precipitates per area is higher.

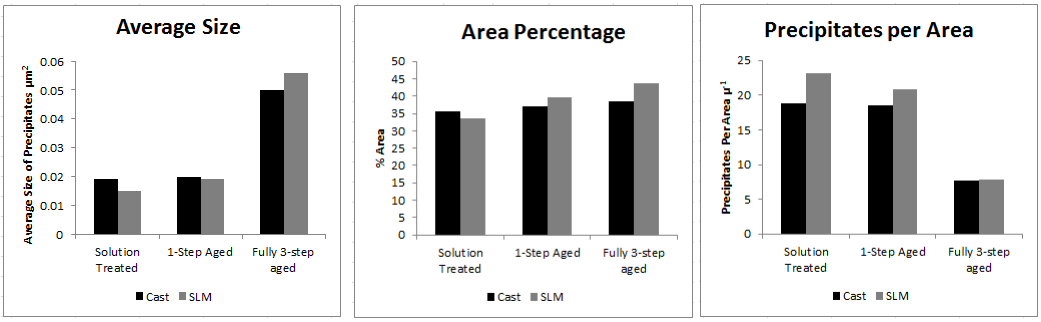

Figure 11: Quantification graphs for gamma prime precipitates in the heat treated materials showing size, area percentage and precipitates per area

CONCLUSIONS

The SLM-produced material has a very different starting microstructure compared to that of the cast material, therefore it is not surprising that the material is affected differently by the heat treatments. In the cast material, some dissolution of carbides occurs, followed by precipitation of new carbides, which then coarsen through the aging steps of the heat treatment, while the grain structure remains unchanged. Whereas in the SLM material, as there are no carbides in the as-produced state, carbides form very quickly during the first step of the heat treatment, and then continue to precipitate up until the end of the heat treatment. Moreover, the microstructure undergoes almost full recrystallization, with the initial high-aspect ratio 'stressed' grains becoming larger, more equi-axed, 'relaxed' grains.

The network of very fine carbides formed during the heat treatment in the SLM-produced material may have a different effect on the mechanical performance in service of the SLM material when compared to the cast materials. A shorter heat treatment may also be beneficial due to the fact that carbides continue to precipitate up until the end of the heat treatment process, meaning that a shorter heat treatment may not have a significant effect if the component is to be used at high temperatures.

The gamma prime structure in the material produced by the two methods is very similar after the heat treatment processes, with slightly larger precipitates in the 3-step aged SLM-produced material which could be beneficial to high temperature performance. However, the tendency of the morphology of the gamma prime precipitates to evolve further, especially in the 1-step aged SLM-produced material suggests that an altered heat treatment may be necessary for this material for optimal performance in service.

ACKNOWLEDGEMENTS

We would like to acknowledge the support of the Engineering and Physical Research Council (EPSRC) for their support for the project - Flexible and Efficient Power Plant: Flex-E-Plant (Grant number: EP/K021095/1). We also thank the following partners for their valuable contributions: GE Power, Doosan Babcock Limited, Centrica plc., EDF Energy (West Burton Power) Limited., Uniper Technology Limited, Goodwin Steel Castings Limited, NPL Management Limited, R-MC Power Recovery Limited., RWE Generation UK plc., Scottish and Southern Energy (SSE) plc., Siemens Industrial Turbomachinery, and TWI Limited. We also acknowledge the support of the Loughborough Materials Characterisation Centre (LMCC).

REFERENCES

[1] Durand-Charre M. The Microstructure of Superalloys. 1st ed. Amsterdam: Gordon and Breach Science Publishers; 1997.

[2] Kleinschmidt A. Additive Manufacturing: From Powders to Finished Products [Internet]. Available from: http://www.siemens.com/innovation/en/home/pictures-of-the-future/industry-and-automation/additive-manufacturing-from-powders-to-finished-products.html

[3] Bi G, Gasser A. Restoration of Nickel-Base Turbine Blade Knife-Edges with Controlled Laser Aided Additive Manufacturing. Phys Procedia [Internet]. 2011 Jan;12:402–9.

[4] Han J, Wright LM. 4.2.2.2: Enhanced Internal Cooling of Turbine Blades and Vanes [Internet]. National Energy Technology Gas Turbine HandbookHan, J., & Wright, L. M. (2006). 4.2.2.2: Enhanced Internal Cooling of Turbine Blades and Vanes. National Energy Technology Gas Turbine Handbook. Retrieved June 2, 2016, from https://www.netl.doe.gov/File Lib. 2006 [cited 2016 Jun 2]. p. 321–52.

[5] Leuders S, Thöne M, Riemer A, Niendorf T, Tröster T, Richard HA, et al. On the mechanical behaviour of titanium alloy TiAl6V4 manufactured by selective laser melting: Fatigue resistance and crack growth performance. Int J Fatigue [Internet]. 2013 Mar [cited 2014 Oct 26];48:300–7.

[6] Kruth JP, Froyen L, Van Vaerenbergh J, Mercelis P, Rombouts M, Lauwers B. Selective laser melting of iron-based powder. J Mater Process Technol [Internet]. 2004 Jun;149(1-3):616–22.

[7] Dinda GP, Dasgupta AK, Mazumder J. Laser aided direct metal deposition of Inconel 625 superalloy: Microstructural evolution and thermal stability. Mater Sci Eng A [Internet]. 2009 May;509(1-2):98–104.

[8] Yavari SA, Wauthle R, van der Stok J, Riemslag AC, Janssen M, Mulier M, et al. Fatigue behavior of porous biomaterials manufactured using selective laser melting. Mater Sci Eng C Mater Biol Appl [Internet]. 2013 Dec;33(8):4849–58.

[9] Mercelis P, Kruth J-P. Residual stresses in selective laser sintering and selective laser melting. Rapid Prototyp J [Internet]. 2006;12(5):254–65.

[10] Thijs L, Montero Sistiaga ML, Wauthle R, Xie Q, Kruth J-P, Van Humbeeck J. Strong morphological and crystallographic texture and resulting yield strength anisotropy in selective laser melted tantalum. Acta Mater [Internet]. 2013 Jul;61(12):4657–68.

[11] Kanagarajah P, Brenne F, Niendorf T, Maier HJ. Inconel 939 processed by selective laser melting: Effect of microstructure and temperature on the mechanical properties under static and cyclic loading. Mater Sci Eng A [Internet]. 2013 Dec;588:188–95.

[12] Qi H, Azer M, Ritter a. Studies of Standard Heat Treatment Effects on Microstructure and Mechanical Properties of Laser Net Shape Manufactured INCONEL 718. Metall Mater Trans A [Internet]. 2009 Aug 14 [cited 2015 Jan 10];40(10):2410–22.

[13] Jahangiri MR, Abedini M. Effect of long time service exposure on microstructure and mechanical properties of gas turbine vanes made of IN939 alloy. Mater Des [Internet]. 2014 Dec [cited 2015 Nov 11];64:588–600.

[14] Thijs L, Verhaeghe F, Craeghs T, Humbeeck J Van, Kruth J-P. A study of the microstructural evolution during selective laser melting of Ti–6Al–4V. Acta Mater [Internet]. 2010 May;58(9):3303–12.
[15] Chen J, Xue L. Process-induced microstructural characteristics of laser consolidated IN-738 superalloy. Mater Sci Eng A [Internet]. 2010 Oct;527(27-28):7318–28.
[16] Sims C., Hagel W. The Superalloys. New York: Wiley; 1972.
[17] Gibbons TB, Stickler R. IN939: Metallurgy, Properties and Performance. High Temp Alloy Gas Turbines [Internet]. 1982;369–93.
[18] Sjöberg G, Imamovic D, Gabel J, Caballero O, Brooks JW, Ferté J, et al. Evaluation of the IN 939 Alloy for Large Aircraft Engine Structures. Superalloys [Internet]. 2004. p. 441–50.
[19] Donachie MJ., Donachie SJ. Superalloys: A Technical Guide. 2nd ed. OH, USA: ASM International; 2002.
[20] Li J, Yuan C, Guo J, Hou J, Zhou L. Effect of hot isostatic pressing on microstructure of cast gas-turbine vanes of K452 alloy. Prog Nat Sci Mater Int. 2014 Dec;24(6):631–6.
[21] Aboulkhair NT, Everitt NM, Ashcroft I, Tuck C. Reducing porosity in AlSi10Mg parts processed by selective laser melting. Addit Manuf [Internet]. 2014 Oct [cited 2014 Dec 26];1-4:77–86.
[22] Tomus D, Jarvis T, Wu X, Mei J, Rometsch P, Herny E, et al. Controlling the Microstructure of Hastelloy-X Components Manufactured by Selective Laser Melting. Phys Procedia [Internet]. 2013 Jan;41:823–7.
[23] Carter LN, Attallah MM, Reed RC. Laser Powder Bed Fabrication of Nickel-Base Superalloys: Influence of Parameters; Characterisation, Quantification and Mitigation of Cracking. Superalloys 2012 [Internet]. John Wiley & Sons, Inc.; 2012. p. 577–86.
[24] Mišković Z, Jovanović M, Gligić M, Lukić B. Microstructural investigation of IN 939 superalloy. Vacuum [Internet]. 1992 May [cited 2015 Feb 10];43(5-7):709–11.
[25] Sims C, Stoloff N, Hagel W. Superalloys II. New York: Wiley; 1987.
[26] Dong X, Zhang X, Du K, Zhou Y, Jin T, Ye H. Microstructure of Carbides at Grain Boundaries in Nickel Based Superalloys. J Mater Sci Technol. The Chinese Society for Metals; 2012;28(11):1031–8.